

A peer-reviewed version of this preprint was published in PeerJ on 27 June 2017.

[View the peer-reviewed version](https://doi.org/10.7717/peerj.3432) (peerj.com/articles/3432), which is the preferred citable publication unless you specifically need to cite this preprint.

Fernández-Calleja V, Hernández P, Schvartzman JB, García de Lacoba M, Krimer DB. 2017. Differential gene expression analysis by RNA-seq reveals the importance of actin cytoskeletal proteins in erythroleukemia cells. PeerJ 5:e3432 <https://doi.org/10.7717/peerj.3432>

Differential gene expression analysis by RNA-seq reveals the importance of actin cytoskeletal proteins in leukemia cells

Vanessa Fernández-Calleja¹, Pablo Hernández¹, Jorge B Schwartzman¹, Dora B Krimer^{Corresp. 1}

¹ Department of Cellular and Molecular Biology, Centro de Investigaciones Biológicas, Spanish National Research Council (CSIC), Madrid, Spain

Corresponding Author: Dora B Krimer

Email address: dbkrimer@cib.csic.es

Development of drug resistance limits the effectiveness of anticancer treatments. Understanding the molecular mechanisms triggering this event in tumor cells may lead to improved therapeutic strategies. Here we used RNA-seq to compare the transcriptomes of an erythroleukemia progenitor cell line (MEL-DS19) and a derived cell line with induced resistance to differentiation (MEL-R). RNA-seq analysis identified a total of 596 genes that were differentially expressed by more than two-fold, of which 486 genes were up-regulated in MEL-DS19 cells and 110 up-regulated in MEL-R cells. These observations revealed that the number of genes expressed in the parental cell line decreased as the cells acquired the resistant phenotype. Clustering analysis of a group of genes showing the highest differential expression allowed identification of a sub-group among genes up-regulated in MEL cells. These genes are related with the organization of the actin cytoskeleton network. Moreover, the majority of these genes are preferentially expressed in the hematopoietic lineage and at least three of them, Was (Wiskott Aldrich syndrome), Btk (Bruton tyrosine kinase) and Rac2, when mutated in humans, give rise to severe hematopoietic deficiencies. Among the group of genes that were up-regulated in MEL-R cells, a significant percentage (16%) corresponded to genes coding for histone proteins, both canonical and variants. A potential implication of these results on the blockade of differentiation in resistant cells is discussed.

Title: "Differential Gene Expression Analysis by RNA-seq Reveals the Importance of Actin Cytoskeletal Proteins in Leukemia Cells"

Authors: Vanessa Fernández-Calleja¹, Pablo Hernández¹, Jorge B. Schwartzman¹ and Dora B. Krimer^{1#}

Address: ¹Department of Cellular and Molecular Biology, Centro de Investigaciones Biológicas (CSIC), Ramiro de Maeztu 9, 28040-Madrid, Spain

Running Title: Differential Expression in Leukemia Cells

Key words: RNA-seq / leukemia cells / cell differentiation / HMBA-resistant / cytoskeleton proteins / Wiskott-Aldrich syndrome / Bruton's tyrosine kinase /

#Corresponding author: Dora B. Krimer

Phone: (+34) 91 837 3112 ext. 4238

Fax: (+34) 91 536 0432

E-mail: dbkrimer@cib.csic.es

22 Abstract

23

24 Development of drug resistance limits the effectiveness of anticancer treatments. Understanding
25 the molecular mechanisms triggering this event in tumor cells may lead to improved therapeutic
26 strategies. Here we used RNA-seq to compare the transcriptomes of an erythroleukemia
27 progenitor cell line (MEL-DS19) and a derived cell line with induced resistance to differentiation
28 (MEL-R). RNA-seq analysis identified a total of 596 genes that were differentially expressed by
29 more than two-fold, of which 486 genes were up-regulated in MEL-DS19 cells and 110 up-
30 regulated in MEL-R cells. These observations revealed that the number of genes expressed in the
31 parental cell line decreased as the cells acquired the resistant phenotype. Clustering analysis of a
32 group of genes showing the highest differential expression allowed identification of a sub-group
33 among genes up-regulated in MEL cells. These genes are related with the organization of the
34 actin cytoskeleton network. Moreover, the majority of these genes are preferentially expressed in
35 the hematopoietic lineage and at least three of them, Was (Wiskott Aldrich syndrome), Btk
36 (Bruton tyrosine kinase) and Rac2, when mutated in humans, give rise to severe hematopoietic
37 deficiencies. Among the group of genes that were up-regulated in MEL-R cells, a significant
38 percentage (16%) corresponded to genes coding for histone proteins, both canonical and variants.
39 A potential implication of these results on the blockade of differentiation in resistant cells is
40 discussed.

Introduction

Cancer cells are distinguished from their normal counterparts by several hallmarks, including uncontrolled growth, lack of response to apoptotic signals and blockade of differentiation [1, 2]. These characteristics serve as a framework for testing different protocols aimed to eliminate tumor cells by aggressive chemotherapy or radiotherapy. Alternatively, cancer cells may be forced to resume the process of maturation by differentiation agents, which generally have less toxicity than conventional cancer treatments. An example of a successful clinical application of differentiation therapy is all-trans-retinoic acid (ATRA) for treatment of acute promyelocytic leukemia, which induces terminal differentiation of promyelocytic leukemic cells [3]. Other differentiation-inducing agents, such as histone-deacetylase (HDAC) inhibitors [4], cytidine analogs (e.g., 5'-aza-2'-deoxycytidine) [5], and tyrosine kinase inhibitors (e.g., imatinib) [6] have been less successful in the treatment of leukemias and tumors. An obstacle to all cancer therapy, including ATRA, is the acquisition of drug resistance that develops in response to repeated therapy and inevitably leads to relapse in most patients, forcing the combination of treatments with additional toxic chemotherapy [7].

In vitro differentiation models have proved to be extremely useful to study the molecular events associated with the blockade of cell differentiation exhibited by some tumor cells and the requirements for re-entry into the cell differentiation program. The erythroleukemia model (MEL cells) developed by Friend and colleagues [8] is an outstanding example that remains as a solid platform to evaluate tumor cell reprogramming after more than 40 years since its description.

Friend erythroblasts are derived from mice infected with the Friend complex virus. Insertion of the Friend spleen focus-forming virus (SFFV) several kilobases upstream of the PU.1/Sfpi1 locus initiation start site leads to its constitutive activation, resulting in a block of erythroid differentiation and the development of erythroleukemia. We have previously reported the establishment of hexamethylene bisacetamide (HMBA)-resistant cell lines (MEL-R) after months of MEL cell culture under pressure with the differentiation inducer, resulting in a cell line that retains most of the parental characteristics [9]. Unexpectedly, we found that PU.1/Sfpi1 remains silent even though MEL-R cells do not differentiate, and this silencing persists in the

presence of chemical inducers other than HMBA. Nevertheless, the SFFV integration site maps exactly to the same location both in the parental MEL and in MEL-R cell lines (2,976 bp downstream of the URE distal element). We also showed that inactivation of PU.1/Sfpi1 in the resistant MEL-R cell line was mediated by DNA methylation at the promoter near to CpG islands [10]. For all these reasons, we believe MEL-R cells might constitute a useful model to study mechanisms that trigger inducer-resistant cell differentiation. Here we compared the differential expression profiles of MEL and MEL-R cells using RNA-seq to identify sequences potentially involved in the control of HMBA resistance. Our results revealed that a higher proportion of differentially-expressed genes are up-regulated in MEL parental cells than in MEL-R cells, with less than 25% of the up-regulated genes in MEL-R, implying a general decline in gene expression concomitant with the gain of the resistant phenotype. Interestingly, a group of highly up-regulated sequences in MEL cells corresponded to genes encoding actin cytoskeleton proteins, whereas a significant proportion of genes up-regulated in MEL-R cells belonged to histone coding genes. Thus, our results pointed to an involvement of the actin cytoskeleton network associated with the acquisition of resistance to HMBA-induced differentiation. A potential contribution of histone gene expression to the differentiation block is also discussed.

Materials and Methods

Cell cultures and treatment

MEL-DS19 (hereafter called MEL) were obtained from Arthur Skoultschi (Albert Einstein College of Medicine, New York, USA). MEL-resistant (hereafter called MEL-R) derived from MEL-DS19, previously established in our lab. Cells were cultured in Dulbecco's modified Eagle's medium containing 10% fetal bovine serum, 100 units/ml penicillin and 100 mg/ml streptomycin (Gibco). Cell differentiation was induced by exposing logarithmically growing cell cultures to 5 mM HMBA. MEL-R cells were routinely cultured in the presence of the differentiation inducer. Hemoglobinized cells were monitored by determining the proportion of benzydine-staining positive cells (B⁺) in the culture.

RNA isolation and RNA-seq

Total RNA was isolated from 1×10^7 cells using the RNeasy kit (Qiagen, Hilden, Germany). DNase I was used to degrade any possible DNA contamination. In total, 1 mg was used to prepare standard RNA-seq libraries (TruSeq RNA Sample Preparation Kit, Illumina, San Diego, CA) based on polyA⁺ isolation. RNA concentration ranged from 326 to 394 ng/ml, and samples showed optimal integrity with RIN values of 9.80. The libraries had an average length of 337–367 nt and were quantified by quantitative PCR (Kapa Biosystems, Woburn, MA) using a previously quantified library as standard. Samples were loaded onto a lane of a flowcell using the Cluster Station apparatus (Illumina) and sequenced on the Illumina GAIIx platform (Parque Científico de Madrid, Spain) under a single read (1×75) protocol. Reads were quality filtered, producing approximately 25 million and 17 million pass filter reads for MEL and MEL-R libraries, respectively, which were used for further bioinformatics analysis. Sequence reads were mapped to a reference mouse genome (NCBI) with TopHat v2.0.1 and further analyzed by DESeq and Cufflinks v2.0.0 to identify differentially expressed transcripts [11].

Quantitative real-time PCR validation

Quantitative real-time-PCR (qRT-PCR) was used to validate the relative expression of genes selected from the RNA-seq analysis. Total RNA was extracted from 1×10^7 MEL and MEL-R cells as described above. In total, 2 mg of isolated RNA was transcribed to cDNA using random hexamers and 200 U of SuperScriptII Reverse Transcriptase (Invitrogen). Reactions were performed in triplicate using the SYBR Green Supermix (Bio-Rad) on an iQ5 System (Bio-Rad, Hercules, CA). The conditions for the amplification were as follows: pre-denaturing step of 95°C for 3 min followed by 40 cycles of 95°C for 30 sec and 60°C for 30 sec, and a final ramp step of 1°C/10 sec from 60°C to 94°C. The primer sequences were designed with Primer3 software (<http://bioinfo.ut.ee/primer3-0.4.0/>) [12] and are listed in S1 Table (for actin cytoskeleton genes), S2 Table (for histone genes) and S3 Table (for methylases and demethylases). Relative gene expression was analyzed by the $2^{-\Delta\Delta Ct}$ method as described [13].

Antibodies and immunoblotting

Control 3T3 fibroblast cells, MEL and MEL-R cells (2.5×10^6) were harvested, washed with PBS and lysed with NP-40 buffer (20 mM Tris-HCl pH 7.5, 10% glycerol, 137 mM NaCl, 1% NP-40, 1 mM sodium orthovanadate, 10 mM sodium fluoride, 2 mM EDTA) containing protease

inhibitors (all from Sigma). Protein lysates (10–30 mg) were separated by 12% SDS-polyacrylamide gel electrophoresis and transferred to PVDF membranes (Bio-Rad). The membranes were incubated with a mouse monoclonal anti- β -actin antibody (1:10000, Sigma) and a rabbit polyclonal anti- α -tubulin antibody (1:1000, ABclonal) followed by five washing steps with T-TBS (20 mM Tris-HCl, 150 mM NaCl, 0.1% Tween 20). Primary antibodies were detected by incubating with HRP-conjugated anti-mouse (1:3000, Santa Cruz) or anti-rabbit IgG (1:1000, DAKO) followed by five cycles of T-TBS washes.

Bisulfite sequencing

The analysis of Btk, Plek and Was promotor regions in MEL, MEL-R and differentiated MEL cells was performed by sodium bisulfite conversion. Genomic DNA from 8×10^4 cells was bisulfite modified using the EZ DNA Methylation-Direct Kit (Zymo Research). Four microlitres of treated DNA was amplified by PCR using primers specific to the bisulfite-converted DNA for each promotor region with ZymoTaq DNA Polymerase (Zymo Research). The conditions for the PCR were as follows: pre-denaturing step of 95°C for 10 min, followed by 40 cycles of 95°C for 30 sec, 55–60°C for 40 sec and 72°C for 40 sec, with a final extension at 72°C for 7 min. The primer sequences were designed using MethPrimer software (<http://www.urogene.org/cgi-bin/methprimer/methprimer.cgi>) [14]. The primers are listed in S4 Table. PCR products were resolved in 1% agarose gels followed by sequencing for methylation analysis, which was performed by Secugen SL (CIB, Madrid).

Cell cycle analysis

Cells (2×10^5 – 1×10^6) were harvested and fixed in 70% ethanol at 4°C for 30 min. Fixed cells were washed twice in PBS and stained with propidium iodide/RNase solution (Immunostep) for 15 min at room temperature (RT). Cell cycle analysis was performed on a Coulter XL flow cytometer and DNA content was analyzed with FlowJo software.

Immunocytochemistry and confocal microscopy

Cells were plated on poly-L-lysine coated slides and incubated at 37°C for 30 min. Cells were fixed with 4% paraformaldehyde for 30 min, permeabilized with 0.1% Triton-X 100 in PBS for 30 min and blocked with 1% bovine serum albumin in PBS/0.1% Triton-X 100 for 1h, all at RT.

Cells were stained with an anti- β -actin antibody (Sigma) for 1h at RT followed by washing twice with PBS. The primary antibody was detected with an Alexa Fluor 568 secondary antibody (Molecular Probes) and 1 μ g/ml DAPI to stain nuclei, for 1h at RT followed by two washes with PBS. Finally, cells were mounted on a cover slip with Prolong Diamond Antifade Mountant reagent (Invitrogen). Fluorescence images were acquired on a Leica TCS SP2 confocal microscope using a 100 \times objective and zoom.

Data access

The raw data files generated by RNA-seq have been deposited in the Gene Expression Omnibus (GEO) database, www.ncbi.nlm.nih.gov/geo (accession no. GSE83567).

Results

Differential gene expression between MEL and MEL-R

We took a genetic approach to identify potential sequences involved in HMBA resistance by using RNA-seq to compare the transcriptomes of MEL and MEL-R cells. The total number of single-end reads generated from each sample was 25 million for MEL and 17 million for MEL-R, 75 nt length in both cases. Samples were further analyzed using the DESeq package for R Statistical Analysis [15]. The trimmed sequencing reads were mapped to the mouse reference genome (Mus_musculus_NCBI_build37.2). Transcript abundance was processed using Cufflinks software suite v2.0.0 [11] and measured as fragments per kb of exon per million fragments mapped (FPKM); the expression level of each transcript was plotted as shown in Fig 1.

Five hundred and ninety-six transcripts were differentially expressed by more than two-fold between MEL and MEL-R cells, of which 486 genes were up-regulated in MEL cells and 110 were up-regulated in MEL-R cells. Values less than two-fold were ignored and matched the gap observed in the curve of Fig 1. Overall, the total number of genes expressed in the parental cell line decreased as the cells acquired the resistant phenotype. We focused our attention on sequences that were highly differentially expressed in MEL relative to MEL-R cells. Fig 2A illustrate the heat map that includes all the genes with a differential expression greater than 2-

fold. An expanded heat map of genes showing highest fold-change values is shown in Fig 2B. PU.1/Sfpi1 was one of the selected genes that, as we demonstrated previously [9], is not expressed in the resistant cell line and served in this case as a positive control for the RNA-seq efficiency.

Searching for common features among the cohort of highly expressed genes in MEL cells, we found that several sequences were implicated in the regulation of the actin cytoskeleton organization. Table 1 lists the groups of genes with the highest expression difference between MEL and MEL-R cell lines. In addition to their relationship with the actin pathway, a good number of these genes were specific to the hematopoietic lineage and at least three of them, WAS (Wiskott Aldrich syndrome), Btk (Bruton tyrosine kinase) and Rac2, when mutated in humans, give rise to severe deficiencies [16-18]. The majority of these genes were mostly linked to the lymphoid or myeloid lineages, and fewer were reported in an erythroid context [19].

From the 110 selected genes whose expression was higher in MEL-R cells than in the progenitor cell line, a large proportion corresponded to genes encoding histone proteins (16%), mostly canonical but also variant histone types. An expanded heat map illustrating the differential gene expression of histones in MEL-R vs MEL cell lines is shown in Fig 2C. Canonical histone proteins H1, H2A, H2B, H3 and H4, are replication-dependent and their expression is coordinated with DNA replication, occurring primarily during the S phase of the cell cycle. There are nonallelic variants mainly of the H1, H2A, H2B and H3 histones that are not restricted in their expression to the S phase and have different physiological roles. Both groups, however, are essential elements of the nucleosome architecture and contribute to chromatin organization. The RNA-seq data revealed differences in the expression of histones that belong to canonical H1, H2A, H2B and H3 groups, and to the variant histones H1f0, H2afx and H3f3b. To understand the significance of the unexpected up-regulation of histone gene expression in MEL-R cells, we compared their DNA content with that of undifferentiated and HMBA-differentiated MEL cells by flow cytometry (Fig 3). We found that the pattern of the major cell cycle phases, G1 vs S vs G2/M, was similar between MEL-R cells and undifferentiated MEL progenitors (MEL-0h). By contrast, differentiated MEL cells (MEL-96h) accumulated at G1, a phenomenon that has been previously observed during MEL cell differentiation [9, 20, 21]. Nevertheless, we

observed that in terms of DNA content, MEL-R cells acquired a tetraploid phenotype as revealed by the shift in DNA content to the right (Fig 3, bottom panel). An increase in the ploidy of MEL-R cell lines might explain the increase in histone gene expression detected by RNA-seq.

Validation of RNA-seq data by qRT-PCR

To validate the results obtained by RNA-seq, we measured the expression fold changes of seven selected genes by qRT-PCR, marked with a red asterisk in Table 1. RNA from MEL cells treated with 5 mM HMBA were included to allow comparison between the undifferentiated and differentiated MEL cells against the resistant MEL-R line. The expression patterns observed in all cases were consistent with the RNA-seq results (Fig 4), confirming the near absence of expression in MEL-R cells. Significant differences were detected, however, when MEL-R cells were compared with MEL cells induced to differentiate with HMBA. Some of the genes such as Was, Rac2, Dock2 or Btk shared a similar expression profile to that obtained in the resistant cell line, showing a tendency toward minimal expression, whereas the expression levels of Plek, Arhgef10l or Nckap1l exhibited either no change or a higher expression than that observed in differentiated cells. These results implied that the gene expression pattern is heterogeneous during differentiation, suggesting that different genes might be involved in distinct pathways, presumably related to cytoskeleton organization.

Validation by qRT-PCR was also performed for histone genes and as before, we included a comparison with HMBA-differentiated MEL cells. The results of the qRT-PCR analysis were in agreement with those of the RNA-seq; in all cases, histone gene expression was higher in MEL-R cells than in MEL cells (Fig 5A), although the difference in the level of expression varied from more than ten-fold (Hist1h2bk) to two-fold (Hist1h2bj). The same pattern was observed between the differentiated (MEL-96h) and undifferentiated samples (Fig 5B). These results ruled out the hypothesis that MEL-R tetraploidy was responsible for histone gene over-expression.

Methylation status of CpG island promoters of Was, Btk and Plek

We have previously demonstrated that PU.1/Sfp1 silencing in MEL-R cells is caused by methylation of nearby CpG islands at its promoter [10]. Moreover, reactivation of silenced

PU.1/Sfpi1 occurs after treatment with 5-aza-2'-deoxycytidine, a potent inhibitor of DNA methylation. To investigate whether DNA methylation is responsible for the down-regulation in gene expression, we examined the methylation status of Btk, Was and Plek promoters in undifferentiated and differentiated MEL cells and in MEL-R cells by bisulfite sequencing. We mapped seven CpG islands upstream of the transcriptional start site of Btk and Was (Fig 6A and B) and five in the case of Plek (Fig 6C). Bisulphite sequencing revealed that all the CpG sites were hypomethylated in undifferentiated (0 h) and differentiated (96 h) MEL cells, whereas the promoters remained hypermethylated at all CpG sites in the resistant cell line. Sites 3, 4 and 5 at the Btk promoter were within a highly cytosine-rich region that were converted to thymine after bisulfite treatment, becoming difficult to resolve. We concluded from these experiments that Btk, Was and Plek expression was silenced by promoter methylation in MEL-R cell lines.

To confirm these results, we examined the expression pattern of the enzymes that catalyze DNA methylation (Dnmt1, Dnmt3a and Dnmt3b) and those that are involved in demethylation processes (Tet1, Tet2 and Tet3). Quantitative RT-PCR analysis revealed that the level of expression of Dnmt1, the maintenance methylase enzyme, was higher in MEL-R cells than in undifferentiated or differentiated MEL cells, whereas minimal changes were detected for the de novo methylases Dnmt3a and Dnmt3b between the different cell populations (Fig 7). By contrast, expression of Tet3, but not Tet1 and Tet2 (enzymes involved in methyl group removal), was markedly reduced in MEL-R cells (Fig 7). These results showed that the increase in DNA methylation by Dnmt1 in MEL-R cells overlaps with a decrease in demethylation by Tet3, which presumably results in the silencing of Btk, Was and Plek promoters.

Actin cytoskeleton is poorly organized in resistant erythroleukemia cells

The actin cytoskeleton is composed of an extensive variety of actin regulators and nucleators that interact through a complicated protein network [22, 23]. Our analysis indicated that the expression of a group of genes related to actin cytoskeleton organization was profoundly depressed in the resistant erythroleukemia cell line. To examine whether actin was affected by the silencing of genes related to actin polymerization and/or regulation, we evaluated its protein expression by Western blotting and found that its levels were similar between MEL and MEL-R cells (Fig 8).

While these results demonstrate that the total amount of actin is equivalent for both cell lines, it does not reveal details of the actin organization. We therefore used fluorescence immunocytochemistry and confocal microscopy with an antibody to actin to localize the protein in fixed MEL and MEL-R cells. In both populations, a rim of actin fluorescence was apparent surrounding nuclei (Fig 9); however, there was an appreciable reduction in signal intensity in MEL-R cells. These results were consistent with the RNA-seq analysis, where a marked reduction in the expression of actin-regulators genes was detected in MEL-R cells, strongly suggesting that actin cytoskeleton organization is perturbed in the resistant erythroleukemia cell line. We hypothesized that proteins of the actin network such as Btk, Was and Plek among others described in Table 1, are essential for such organization although it is unclear whether the absence of expression is a cause or consequence of the defect.

Discussion

Cancer cells can acquire resistance to most traditional chemotherapy regimes and also targeted therapies, and such an occurrence remains a great concern in cancer treatment [24, 25]. Research on molecular and cellular mechanisms that confer resistance to tumor cells is therefore a major focus of basic and clinical investigation. Along this line, cell culture models have been crucial to advance in the understanding of cancer cell resistance. We took advantage of an HMBA-resistant cell line derived from Friend's erythroleukemia cells, previously established in our lab [9, 10], to study the molecular events that contribute to the resistant phenotype. Both MEL and MEL-R cell lines are blocked at the proerythroblast stage of differentiation but unlike the progenitor cell line, MEL-R cells do not react to HMBA or other chemical inducers (e.g., DMSO, hemin and butyrate) and remain resistant against cell differentiation. In the present study, we used RNA-seq technology to identify genes potentially involved in the resistance mechanism. Our analysis identified 596 genes that were differentially expressed between progenitor and resistant cells, with the majority corresponding to genes up-regulated in MEL cells while only 110 were up-regulated in MEL-R cells.

Among these identified genes, some of them were conspicuous by their high differential expression between MEL and MEL-R and for sharing two important features: belonging to the actin regulatory network and being preferentially expressed in the hematopoietic lineage. Moreover, many of these genes are specifically activated in hematopoietic lineages and at least three, Was, Btk and Rac2, when mutated are linked to severe human hematological pathologies [16-18]. Additionally, a recent study showed that biallelic mutations in the Dock2 gene results in severe immunodeficiency that leads to defects in actin polymerization [26].

The network of actin filaments provides mechanical support to the cell cytoskeleton, but it is increasingly acknowledged that it also contributes to other critical cellular processes. Emerging evidence points to a role for the actin cytoskeleton in controlling and regulating receptor signaling [27]. We show here a dramatic down-regulation of some of these network components in MEL-R cells, which correlates well with the methylation status at nearby CpG islands in the promoters of Was, Btk and Plek. Over-expression of the methyltransferase Dnmt1, a maintenance methylase that acts on hemimethylated DNA, and the repression of the Tet3 demethylase, support these findings, leading us to speculate that silencing of most of the cytoskeleton-associated proteins is linked to a hypermethylation status. Interestingly, whereas no significant changes in total actin protein levels were observed between MEL and MEL-R cells, a weaker signal was detected in MEL-R cells by immunocytochemistry, which might suggest poor actin organization. Regulation of actin polymerization in eukaryotes requires a large number of accessory proteins that facilitate polymerization or disassembly of monomeric globular actin (G-actin) into filamentous actin (F-actin) and vice versa; many of these proteins interact with each other. For example, Btk interacts with Was and activates the protein by inducing its phosphorylation in B cells [28]. Btk also promotes a Rac2 response, leading to F-actin rearrangements in mast cells [29]. Dock2 is essential for lymphocyte migration and mediates cytoskeletal reorganization through Rac2 activation [30]. The transcription factor PU.1, responsible for the differentiation block in MEL cells but silenced in MEL-R cells, is a major regulator of Btk expression both in myeloid and lymphoid cells [31, 32]. In summary, the actin cytoskeleton network is orchestrated through multiple associated proteins probably with overlapping roles, which contribute to different cell functions through complex associations. As

we showed here, silencing of some of these proteins has deleterious effects on actin organization and we hazard that this might be a cause for the blockade of differentiation in resistant cells.

As stated earlier, only 110 from 596 differentially-expressed genes were up-regulated in MEL-R cells. This indicates a tendency towards a general shut-down of gene expression in resistant cells, a situation comparable with what occurs during cell differentiation. Silenced compartments composed mainly of heterochromatin are considered hallmarks of the differentiated cells, a condition that progresses all through terminal differentiation (reviewed in [33]. A gradual increase in heterochromatinization has been described in differentiating leukemia cells, as measured by the amount of the heterochromatin-associated HP1a, which increases continuously during MEL terminal differentiation [34]. Heterochromatinization is enhanced in MEL-R cells relative to undifferentiated MEL cells, but is nevertheless lower than in HMBA-differentiated cells (unpublished results). The progressive gene silencing observed in MEL-R cells is one additional element that suggests that these cells are at a midway point between the undifferentiated and differentiated phenotypes due to a block somewhere in the process. Concomitant with this genetic blackout, histone genes emerge as the major group up-regulated in the resistant phenotype. Initially, we associated the histone gene expression pattern with the tetraploid status of the MEL-R cell lines. Polyploidy has been reported in tumor cells as a result of stress-induced endoreplication [35, 36]. Chronic HMBA treatment might represent a hard-hitting stress that MEL-R cells overcome via a survival phenotype, i.e. tetraploidization, increased cell size and impaired cell differentiation. Coward and Harding in a comprehensive perspective support the hypothesis that tetraploidy provides numerous advantages during tumor initiation. [37]. Moreover, they present data sustaining that polyploid facilitates the acquisition of therapy-resistance in multiple cancers. MEL-R tetraploidy may possibly involve chromatin rearrangements and consequently histone gene expression changes. Nevertheless, the same fluctuations in histone gene expression were observed in differentiated cells, indicating that differentiated and resistant cells share a common mechanism. In vivo, the quantity of reticulocytes, a stage comparable to the last stages of HMBA-induced differentiation, increases several fold in a very short time [38], and it is speculated that a large amount of histones needs to be generated. Recently, it was shown that when reticulocytes mature and before enucleation, major histones are released into the cytoplasm from an unexpected nuclear opening during

terminal erythropoiesis, a migration that is crucial for chromatin condensation and terminal differentiation [39]. We speculate that as an increase in histones occur both in HMBA-differentiated MEL and in MEL-R cells, a failure in chromatin condensation, either by an impairment in histone release or by a yet unknown mechanism, might interfere with terminal cell differentiation in resistant cells.

Acknowledgements

We acknowledge María-José Fernández Nestosa for her suggestions and critical reading of the manuscript and Alicia Bernabé for technical help. We are grateful to Mario García and his team from the Bioinformatics and Biostatistics Facility at the CIB for their efficient and dedicated technical support for the Next Generation Sequencing data analysis.

References

- [1] Hanahan D, Weinberg RA. The hallmarks of cancer. *Cell*. 2000 Jan 7;100(1):57-70.
- [2] Hanahan D, Weinberg RA. Hallmarks of cancer: the next generation. *Cell*. 2011 Mar 4;144(5):646-74.
- [3] Nowak D, Stewart D, Koeffler HP. Differentiation therapy of leukemia: 3 decades of development. *Blood*. 2009 Apr 16;113(16):3655-65.
- [4] Lane AA, Chabner BA. Histone deacetylase inhibitors in cancer therapy. *J Clin Oncol*. 2009 Nov 10;27(32):5459-68.
- [5] Fenaux P, Mufti GJ, Hellstrom-Lindberg E, Santini V, Gattermann N, Germing U, et al. Azacitidine prolongs overall survival compared with conventional care regimens in elderly patients with low bone marrow blast count acute myeloid leukemia. *J Clin Oncol*. 2010 Feb 1;28(4):562-9.
- [6] Haouala A, Widmer N, Duchosal MA, Montemurro M, Buclin T, Decosterd LA. Drug interactions with the tyrosine kinase inhibitors imatinib, dasatinib, and nilotinib. *Blood*. 2011 Feb 24;117(8):e75-87.
- [7] Iland HJ, Bradstock K, Supple SG, Catalano A, Collins M, Hertzberg M, et al. All-trans-retinoic acid, idarubicin, and IV arsenic trioxide as initial therapy in acute promyelocytic leukemia (APML4). *Blood*. 2012 Aug 23;120(8):1570-80; quiz 752.
- [8] Friend C, Scher W, Holland JG, Sato T. Hemoglobin synthesis in murine virus-induced leukemic cells in vitro: stimulation of erythroid differentiation by dimethyl sulfoxide. *Proc Natl Acad Sci U S A*. 1971 Feb;68(2):378-82.

- 419 [9] Fernandez-Nestosa MJ, Hernandez P, Schwartzman JB, Krimer DB. PU.1 is dispensable
420 to block erythroid differentiation in Friend erythroleukemia cells. *Leuk Res.* 2008 Jan;32(1):121-
421 30.
- 422 [10] Fernandez-Nestosa MJ, Monturus E, Sanchez Z, Torres FS, Fernandez AF, Fraga MF, et
423 al. DNA methylation-mediated silencing of PU.1 in leukemia cells resistant to cell
424 differentiation. *Springerplus.* 2013;2:392.
- 425 [11] Trapnell C, Roberts A, Goff L, Pertea G, Kim D, Kelley DR, et al. Differential gene and
426 transcript expression analysis of RNA-seq experiments with TopHat and Cufflinks. *Nat Protoc.*
427 2012 Mar;7(3):562-78.
- 428 [12] Untergasser A, Cutcutache I, Koressaar T, Ye J, Faircloth BC, Remm M, et al. Primer3--
429 new capabilities and interfaces. *Nucleic Acids Res.* 2012 Aug;40(15):e115.
- 430 [13] Schmittgen TD, Livak KJ. Analyzing real-time PCR data by the comparative C(T)
431 method. *Nat Protoc.* 2008;3(6):1101-8.
- 432 [14] Li LC, Dahiya R. MethPrimer: designing primers for methylation PCRs. *Bioinformatics.*
433 2002 Nov;18(11):1427-31.
- 434 [15] Anders S, Reyes A, Huber W. Detecting differential usage of exons from RNA-seq data.
435 *Genome Res.* 2012 Oct;22(10):2008-17.
- 436 [16] Ambruso DR, Knall C, Abell AN, Panepinto J, Kurkchubasche A, Thurman G, et al.
437 Human neutrophil immunodeficiency syndrome is associated with an inhibitory Rac2 mutation.
438 *Proc Natl Acad Sci U S A.* 2000 Apr 25;97(9):4654-9.
- 439 [17] Bosticardo M, Marangoni F, Aiuti A, Villa A, Grazia Roncarolo M. Recent advances in
440 understanding the pathophysiology of Wiskott-Aldrich syndrome. *Blood.* 2009 Jun
441 18;113(25):6288-95.
- 442 [18] Conley ME, Dobbs AK, Farmer DM, Kilic S, Paris K, Grigoriadou S, et al. Primary B
443 cell immunodeficiencies: comparisons and contrasts. *Annu Rev Immunol.* 2009;27:199-227.
- 444 [19] Schmidt U, van den Akker E, Parren-van Amelsvoort M, Litos G, de Bruijn M, Gutierrez
445 L, et al. Btk is required for an efficient response to erythropoietin and for SCF-controlled
446 protection against TRAIL in erythroid progenitors. *J Exp Med.* 2004 Mar 15;199(6):785-95.
- 447 [20] Kiyokawa H, Richon VM, Venta-Perez G, Rifkind RA, Marks PA.
448 Hexamethylenebisacetamide-induced erythroleukemia cell differentiation involves modulation of
449 events required for cell cycle progression through G1. *Proc Natl Acad Sci U S A.* 1993 Jul
450 15;90(14):6746-50.
- 451 [21] Vanegas N, Garcia-Sacristan A, Lopez-Fernandez LA, Parraga M, del Mazo J,
452 Hernandez P, et al. Differential expression of Ran GTPase during HMBA-induced differentiation
453 in murine erythroleukemia cells. *Leuk Res.* 2003 Jul;27(7):607-15.
- 454 [22] Bezanilla M, Gladfelter AS, Kovar DR, Lee WL. Cytoskeletal dynamics: a view from the
455 membrane. *J Cell Biol.* 2015 May 11;209(3):329-37.
- 456 [23] Moulding DA, Record J, Malinova D, Thrasher AJ. Actin cytoskeletal defects in
457 immunodeficiency. *Immunol Rev.* 2013 Nov;256(1):282-99.
- 458 [24] Rebucci M, Michiels C. Molecular aspects of cancer cell resistance to chemotherapy.
459 *Biochem Pharmacol.* 2013 May 1;85(9):1219-26.
- 460 [25] Raguz S, Yague E. Resistance to chemotherapy: new treatments and novel insights into
461 an old problem. *Br J Cancer.* 2008 Aug 5;99(3):387-91.
- 462 [26] Dobbs K, Dominguez Conde C, Zhang SY, Parolini S, Audry M, Chou J, et al. Inherited
463 DOCK2 Deficiency in Patients with Early-Onset Invasive Infections. *N Engl J Med.* 2015 Jun
464 18;372(25):2409-22.

- [27] Mattila PK, Batista FD, Treanor B. Dynamics of the actin cytoskeleton mediates receptor cross talk: An emerging concept in tuning receptor signaling. *J Cell Biol.* 2016 Feb 1;212(3):267-80.
- [28] Sharma S, Orlowski G, Song W. Btk regulates B cell receptor-mediated antigen processing and presentation by controlling actin cytoskeleton dynamics in B cells. *J Immunol.* 2009 Jan 1;182(1):329-39.
- [29] Kuehn HS, Radinger M, Brown JM, Ali K, Vanhaesebroeck B, Beaven MA, et al. Btk-dependent Rac activation and actin rearrangement following FcepsilonRI aggregation promotes enhanced chemotactic responses of mast cells. *J Cell Sci.* 2010 Aug 1;123(Pt 15):2576-85.
- [30] Fukui Y, Hashimoto O, Sanui T, Oono T, Koga H, Abe M, et al. Haematopoietic cell-specific CDM family protein DOCK2 is essential for lymphocyte migration. *Nature.* 2001 Aug 23;412(6849):826-31.
- [31] Christie DA, Xu LS, Turkistany SA, Solomon LA, Li SK, Yim E, et al. PU.1 opposes IL-7-dependent proliferation of developing B cells with involvement of the direct target gene bruton tyrosine kinase. *J Immunol.* 2015 Jan 15;194(2):595-605.
- [32] Himmelmann A, Thevenin C, Harrison K, Kehrl JH. Analysis of the Bruton's tyrosine kinase gene promoter reveals critical PU.1 and SP1 sites. *Blood.* 1996 Feb 1;87(3):1036-44.
- [33] Politz JC, Scalzo D, Groudine M. Something silent this way forms: the functional organization of the repressive nuclear compartment. *Annu Rev Cell Dev Biol.* 2013;29:241-70.
- [34] Estefania MM, Ganier O, Hernandez P, Schvartzman JB, Mechali M, Krimer DB. DNA replication fading as proliferating cells advance in their commitment to terminal differentiation. *Sci Rep.* 2012;2:279.
- [35] Lee HO, Davidson JM, Duronio RJ. Endoreplication: polyploidy with purpose. *Genes Dev.* 2009 Nov 1;23(21):2461-77.
- [36] Storchova Z, Pellman D. From polyploidy to aneuploidy, genome instability and cancer. *Nat Rev Mol Cell Biol.* 2004 Jan;5(1):45-54.
- [37] Coward J, Harding A. Size does matter: why polyploid tumor cells are critical drug targets in the war on cancer. *Front Oncol.* 2014;4:123.
- [38] Ji P, Jayapal SR, Lodish HF. Enucleation of cultured mouse fetal erythroblasts requires Rac GTPases and mDia2. *Nat Cell Biol.* 2008 Mar;10(3):314-21.
- [39] Zhao B, Mei Y, Schipma MJ, Roth EW, Bleher R, Rappoport JZ, et al. Nuclear Condensation during Mouse Erythropoiesis Requires Caspase-3-Mediated Nuclear Opening. *Dev Cell.* 2016 Mar 7;36(5):498-510.
- [40] Ward J, Jr. Hierarchical Grouping to Optimize an Objective Function. *Journal of the American Statistical Association.* 1963;8(301):236-44.

Figure 1(on next page)

Differentially expressed transcripts between parental MEL-DS19 (MEL) and HMBA-resistant (MEL-R) cell lines identified by RNA-seq.

Differentially expressed genes were plotted according to fold changes represented by the FPKM ratio in a logarithmical scale. In total, 486 up-regulated genes were identified in the parental line (FPKM MEL > FPKM MEL-R) whereas 110 were up-regulated in the resistant cells (FPKM MEL < FPKM MEL-R). A two-fold change cutoff was applied in both cases reflected by the discontinuity of the curve.

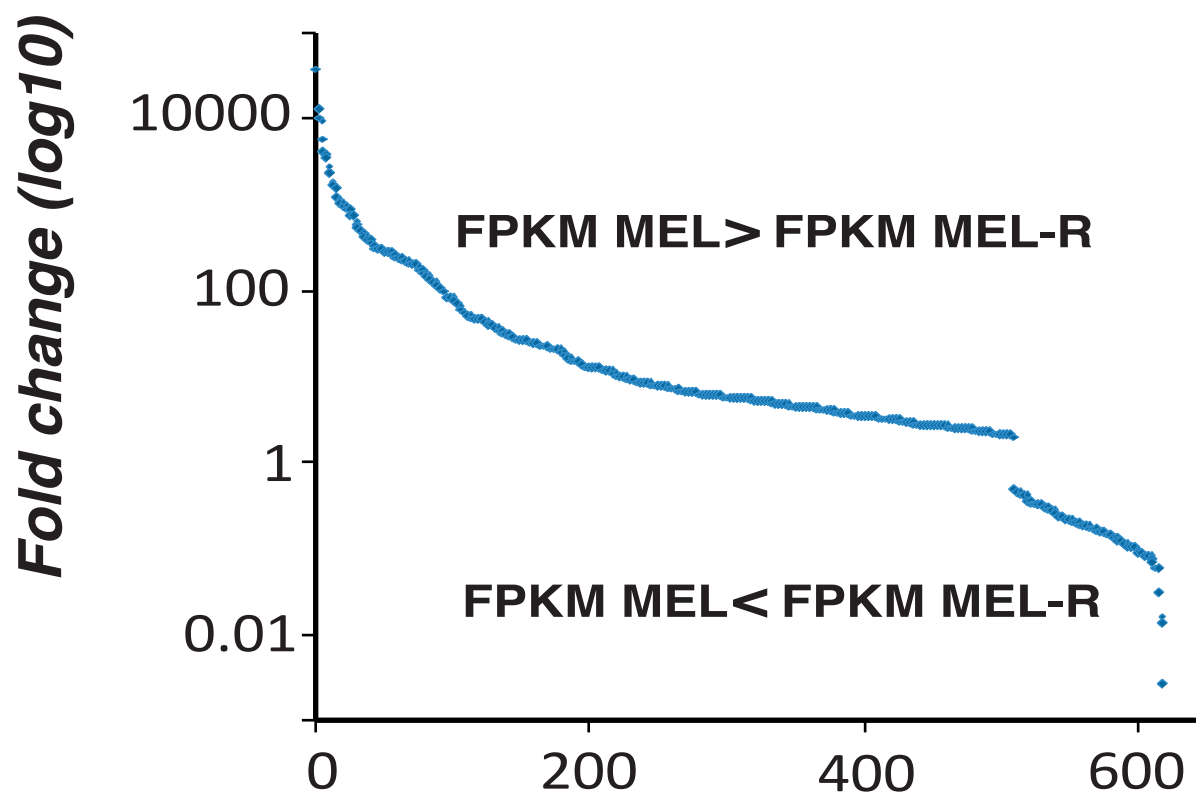


Fig. 1

Figure 2(on next page)

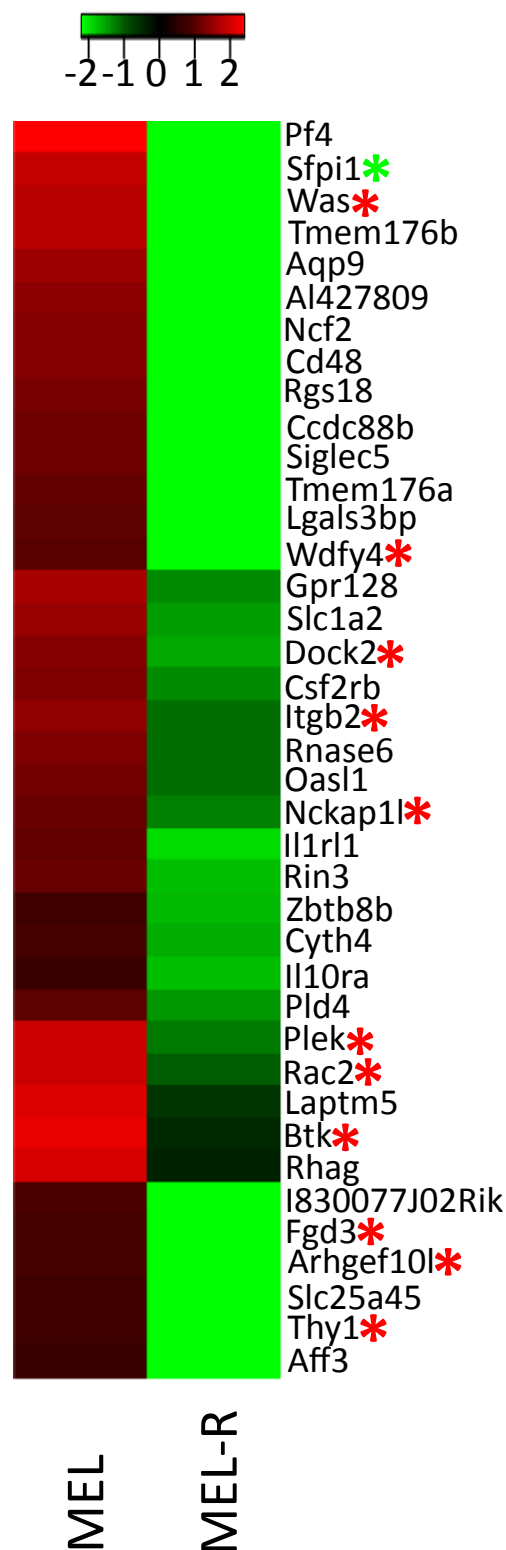
Expression differences between MEL and MEL-R cell lines.

A) Cluster analysis of differentially expressed genes between MEL and MEL-R cell lines classified based on analysis of minimum variance [40] . B) Heat map zoomed to amplify the genes with higher fold-change values. Genes related to the actin cytoskeletal network are indicated by red asterisks. As expected, PU.1/Sfpi presented strong differences in expression towards the progenitor cells and served as control for RNA-seq efficiency (green asterisk). C) Heat map limited to histone gene expression,. Red and green colors represent high and low expression, respectively, for all the panels.

A



B



C



Figure 3(on next page)

Tetraploidy characterizes HMBA-resistant cells.

DNA content assayed by propidium iodide (PI) staining and flow cytometry show that HMBA-induced differentiated MEL cells (MEL-96h) accumulate in G1 as compared with the uninduced cell line (MEL-0h). DNA profile of HMBA-resistant cells (MEL-R) is similar to that observed in uninduced MEL cells regarding the fractions of cells in G1, S and G2-M. However, the DNA content profile is shifted to the right of the panel confirming that those cells become tetraploid.

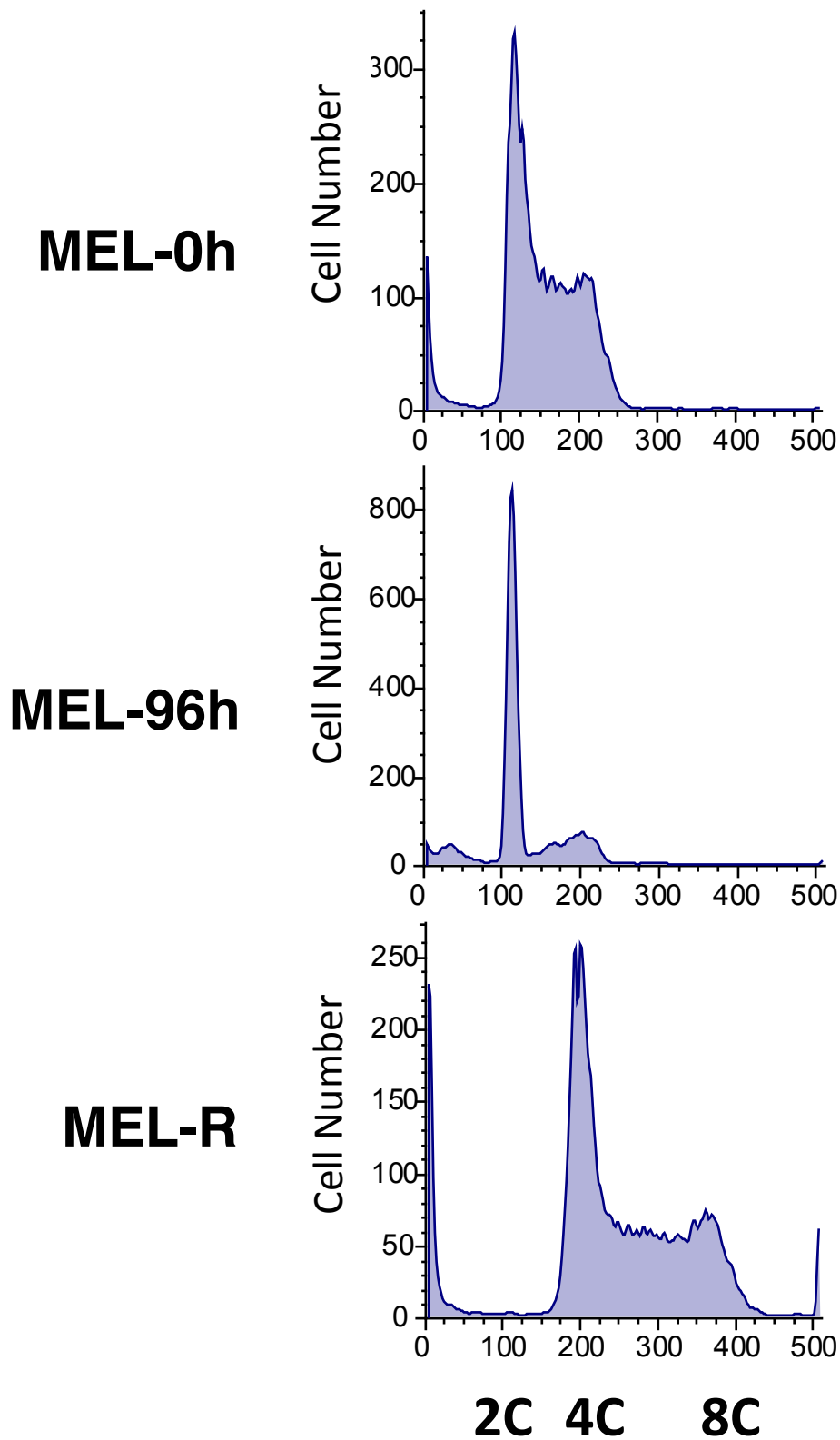


Fig. 3

Figure 4 (on next page)

Validation of differentially regulated genes associated with the actin cytoskeletal network by qRT-PCR.

Selected genes that exhibited the highest FPKM values between MEL and MEL-R cell lines by RNA-seq were chosen for further validation by qRT-PCR. For the progenitor cell line, samples treated with HMBA for 96 h were also included. Data were normalized to b-actin expression for each sample. Bars represent \pm SD of triplicate determinations.

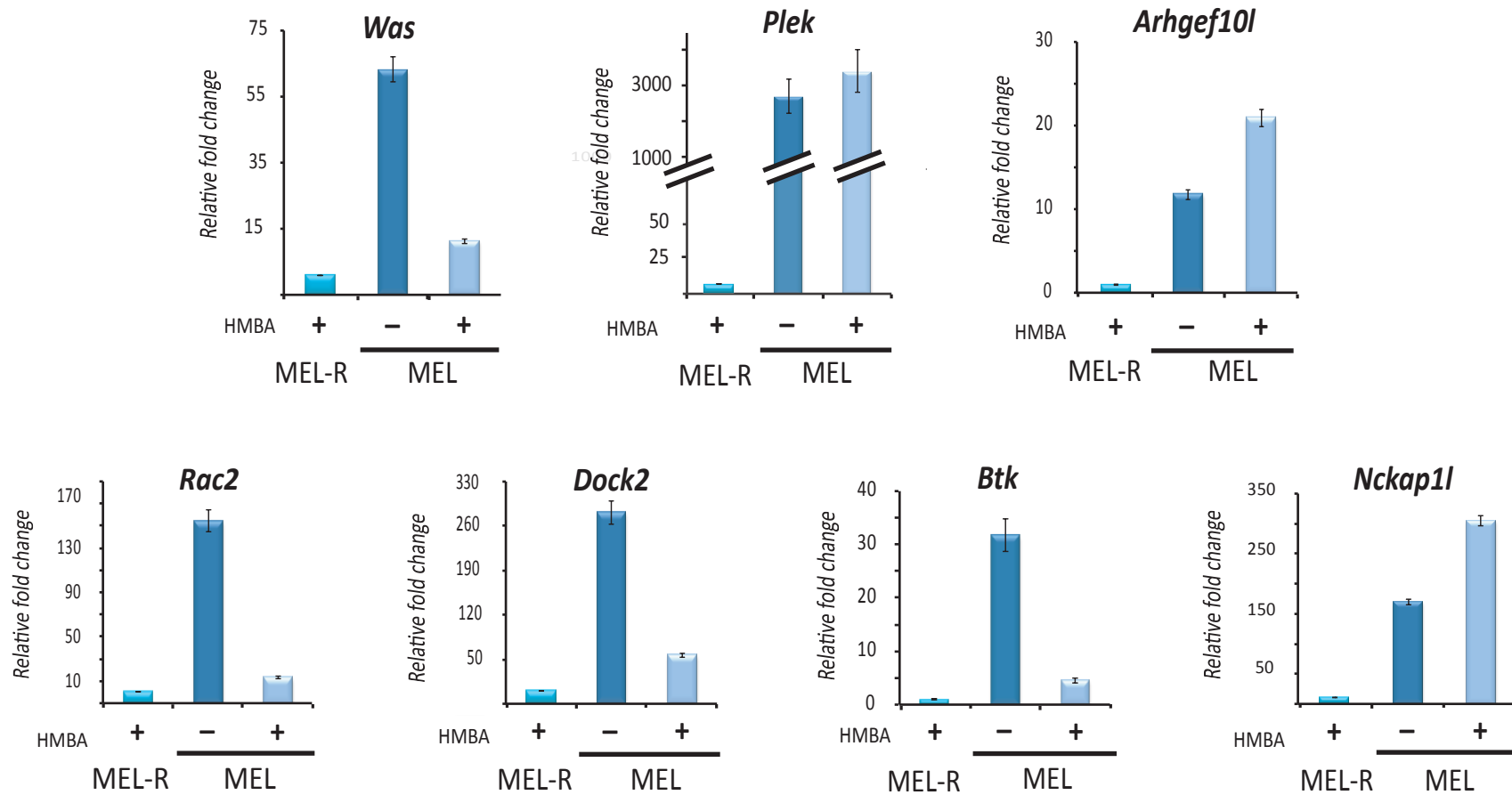


Fig. 4

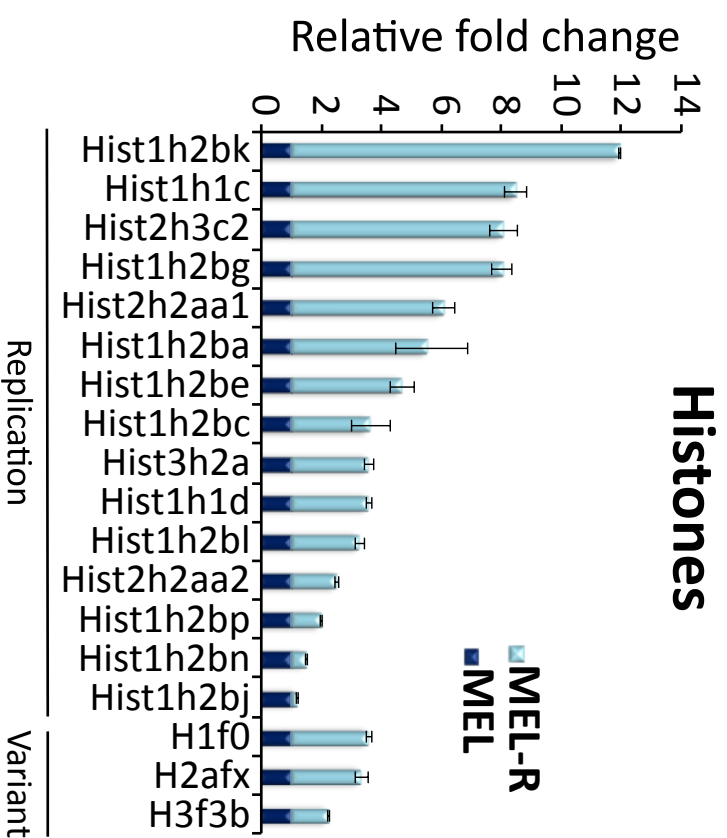
Figure 5 (on next page)

Differential histone gene expression between progenitor and resistant cell lines and after differentiation.

qRT-PCR analysis of histone genes, canonical and variant, up-regulated in MEL-R cells relative to MEL cells, and B) in HMBA-induced MEL cells (MEL 96h) relative to uninduced cells (MEL).

Data were normalized to b-actin expression for each sample. Bars represent \pm SD of triplicate determinations

A



B

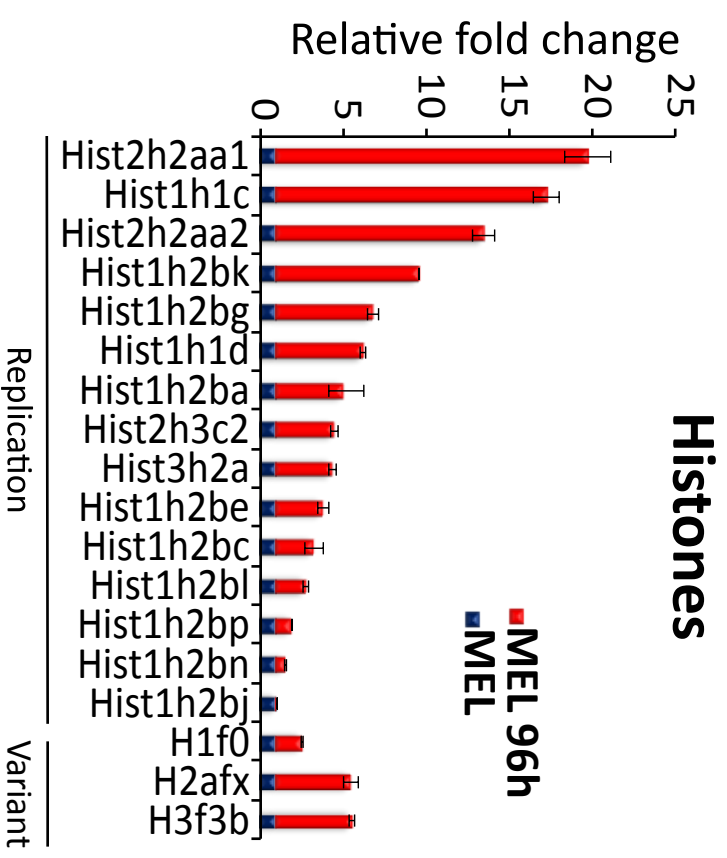


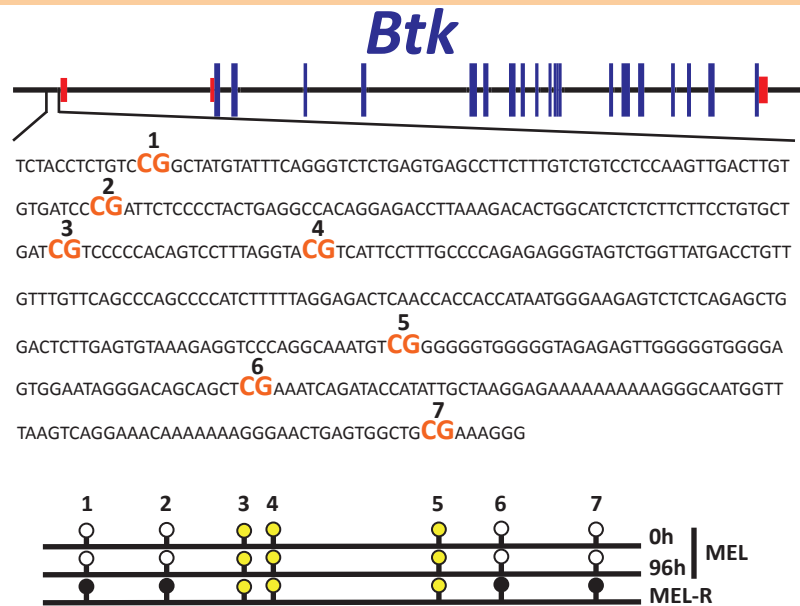
Fig. 5

Figure 6 (on next page)

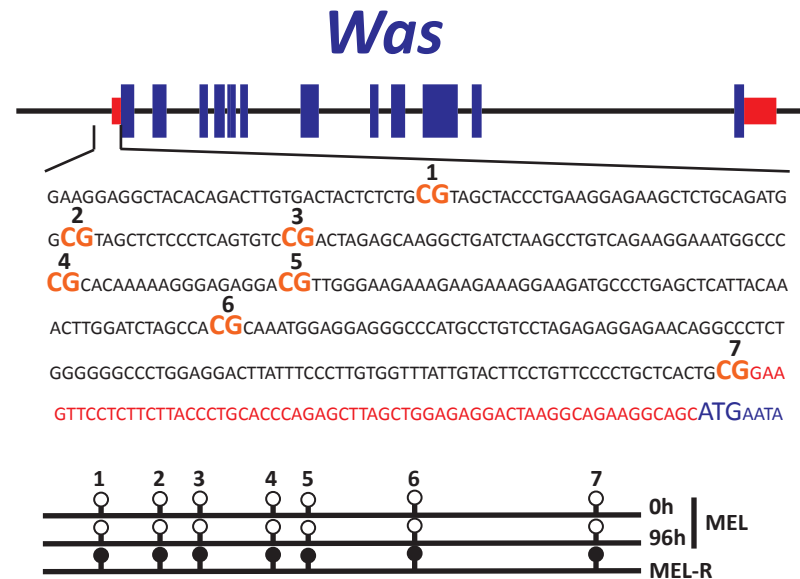
Methylation status of the Btk, Was and Plek promoters at the HMBA-resistant cells.

Genomic maps including exons (blue rectangles) and 5' and 3' UTRs (red rectangles) of A) Btk, B) Was and C) Plek. Expanded regions illustrate the promoter regions containing seven CpG islands (CG) for Btk and Was and five CpG islands for Plek. "Lollipop" schematic diagram of methylation patterns is represented below each sequence. Results from untreated (0h) or HMBA-treated MEL cells (96 h) as well as MEL-R cells are shown. Black and white lollipops indicate methylated or unmethylated CpGs, respectively, while undetermined methylation status (see text for details) is represented in yellow.

A



B



C

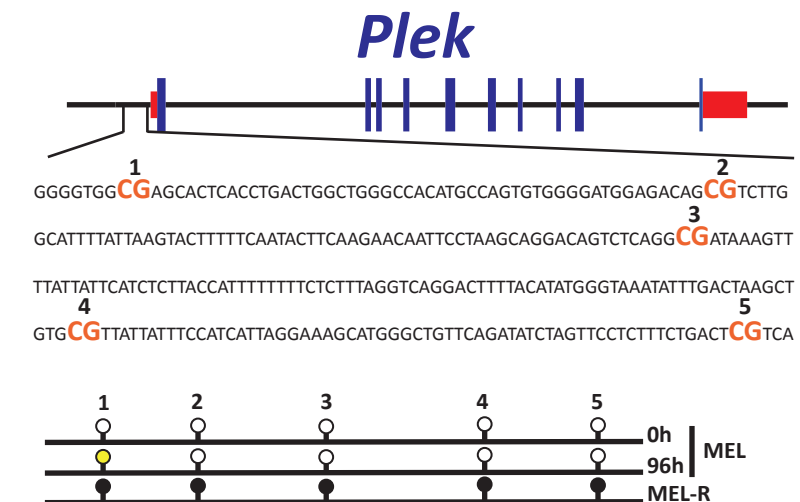


Fig. 6

Figure 7 (on next page)

High and low expression of Dnmt1 and Tet3, respectively, correlate well with gene silencing and DNA methylation in MEL-R cells.

qRT-PCR was performed for Dnmt1, Dnmt3a and Dnmt3b methylases and Tet1, Tet2 and Tet3 demethylases in undifferentiated, HMBA-treated MEL cells and in MEL-R cells. Data were normalized to b-actin expression for each sample. Bars represent \pm SD of triplicate determinations.

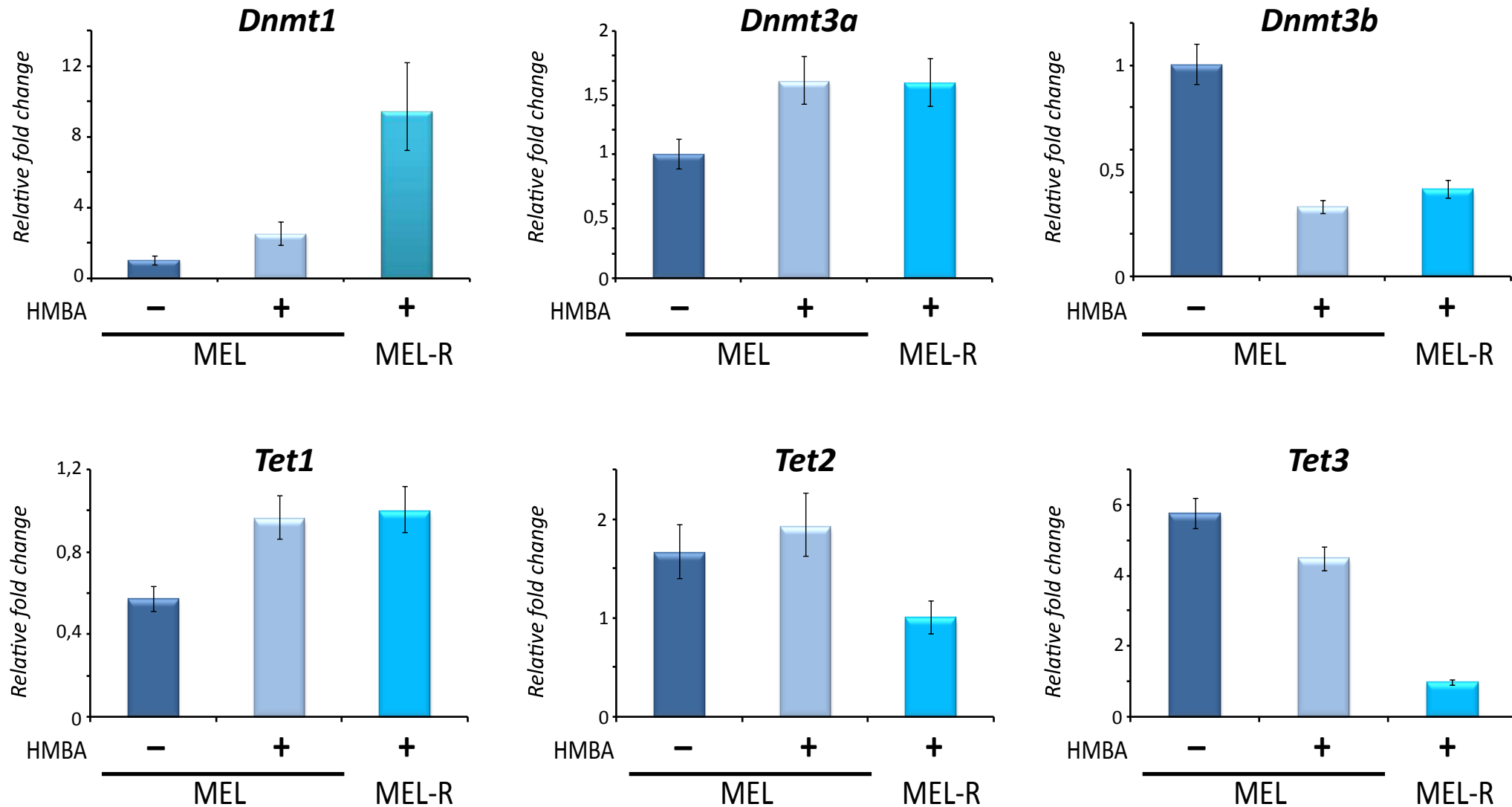


Fig. 7

Figure 8(on next page)

Actin protein is equally abundant in progenitor and resistant MEL cells.

Western blot analysis for actin protein expression in MEL and MEL-R leukemia cells and in 3T3 control fibroblasts. Equal amounts of protein were loaded and immunoblotted with an anti-b-actin antibody. Anti a-tubulin was used as a loading control.

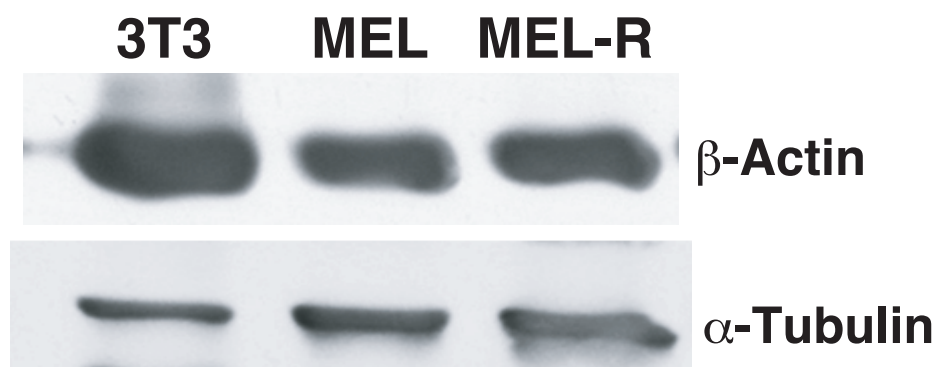


Fig. 8

Figure 9(on next page)

Actin cytoskeleton integrity is perturbed in MEL-resistant cell lines.

Confocal immunofluorescence microscopy of progenitor MEL cells and resistant MEL-R cells stained with a mouse monoclonal anti- β -actin antibody (red). Nuclear DNA was stained with DAPI (blue). Scale bar is 10 μ m.

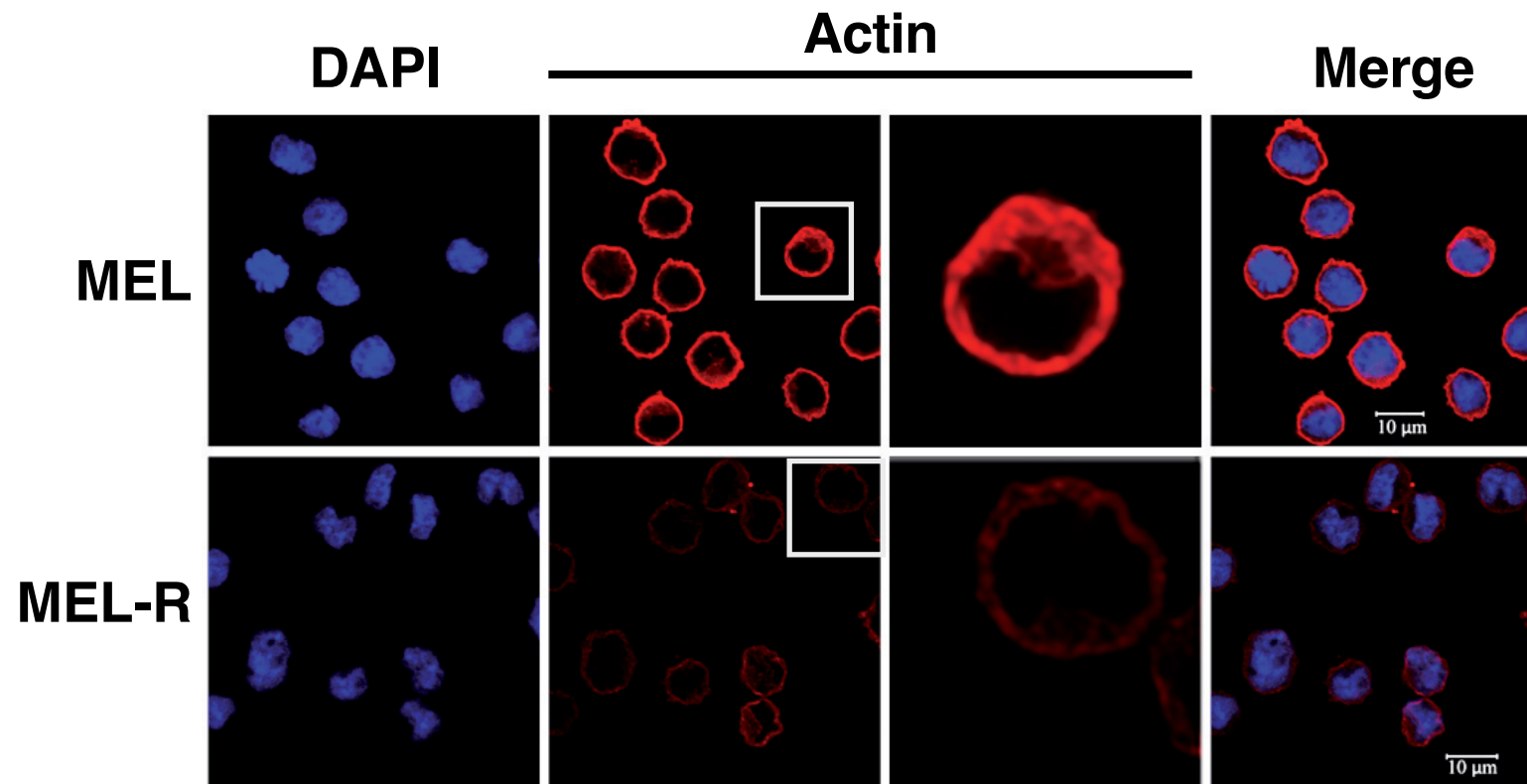


Fig. 9

Table 1(on next page)

List of differentially expressed genes related to actin cytoskeleton

List of differentially expressed genes related to actin cytoskeleton

Table 1. List of differentially expressed genes related to actin cytoskeleton

Gene	Locus	FPKM_MELR	FPKM_MEL	Log2 (Fold Change)
*Was	X:7658591-7667617	0.00631327	65.48	13.3403792
Wdfy4	14:33772732-33998252	0.00631327	9.78436	10.5978743
*Plek	11:16871208-16908721	0.0599941	90.8539	10.5645121
Fgd3	13:49358478-49404577	0.00631327	6.88043	10.0898956
*Arhgef10l	4:140070399-140221820	0.00631327	6.2823	9.95868967
*Rac2	15:78389598-78403213	0.0930802	91.0001	9.9331781
Thy1	9:43851466-43856662	0.00631327	5.54603	9.77885225
*Dock2	11:34126863-34414545	0.0272059	23.2087	9.73653044
*Btk	X:131076879-131117679	0.358226	148.999	8.70021688
Itgb2	10:76993092-77028419	0.0698373	27.2361	8.60730664
*Nckap1l	15:103284255-103329231	0.0550022	13.9085	7.9822618